Orbital
The electronic journal of chemistry

the electronic journal of chemistry

Full Paper | http://dx.doi.org/10.17807/orbital.v13i1.1533

A Computational Investigation of Electronic Structure and Optical Properties of $AlCuO_2$ and $AlCu_{0.96}Fe_{0.04}O_2$: A First Principle Approach

Md. Tawhidul Islam [a], Ajoy Kumer [b], Unesco Chakma [a], Debashis Howlader [a]

The synthesized compound $AlCuO_2$ was established and structurally characterized as the semiconductor. It is noted that there are no available data for theoretical studies, as well as computational studies. For developing theoretical studies on $AlCuO_2$, this study has been designed by computational tools. Applying computational approaches, the electronic structure and optical properties were calculated for the $AlCuO_2$ molecule, and computational tools of the CASTAP code from material studio 8.0 were used in this investigation. First of all, the band gap was recorded by 1.81 eV through the Generalized Gradient Approximation (GGA) based on the Perdew Burke Ernzerhof (PBE), and the density of state and the partial density of state were simulated for evaluating the nature of $3s^2$, $3p^1$ orbital for Al, $3d^{10}$, $4s^1$ orbital for Cu, $3d^6$, $4s^2$ orbital for Fe and $2s^2$, $2p^4$ orbital for O atom of $AlCuO_2$. The optical properties, for instance, absorption, reflection, refractive index, conductivity, dielectric function, and loss function, were calculated. To develop the conducting nature, 4% Fe atom was doped by replacing the Cu atom on $AlCuO_2$. As a result, the band gap was found at 0.00 eV having molecular formulation as $AlCu_{0.96}Fe_{0.04}O_2$, as well as the optical conductivity and optical absorption was soared comparing with parent $AlCuO_2$. From the analysis of the band gap and optical properties in $AlCu_{0.96}Fe_{0.04}O_2$, it can be established that the semiconductor, $AlCuO_2$, has converted into a superconductor due to 4% Fe atom doping.

Graphical abstract

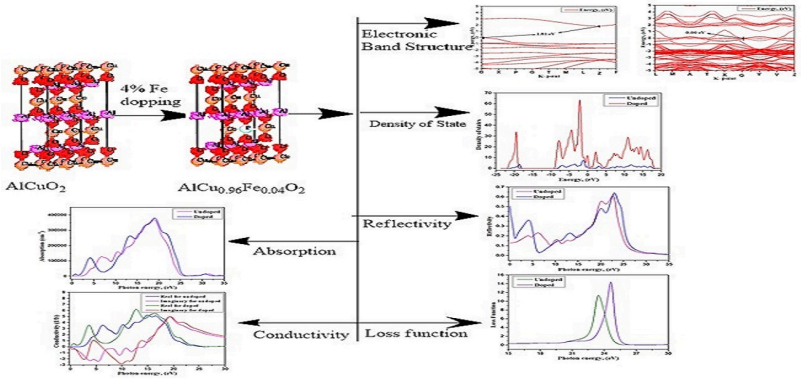

Keywords

Band gap
DOS
Electronic structure
Fe doping
Optical properties
PDOS

Article history

Received: 13 August 2020
Revised: 11 January 2021
Accepted: 25 February 2021
Available online 27 March 2021

Editor: Adilson Beatriz

1. Introduction

With the enlargement of the global semiconductor industry, semiconductor materials are a fundamental element for the information society's high-tech industry, and the 21st century has become a significant data age [1, 2].

[a] Department of Electrical and Electronics Engineering, European University of Bangladesh, Gabtoli, Dhaka-1216, Bangladesh. [b] Department of Chemistry, European University of Bangladesh, Gabtoli, Dhaka-1216, Bangladesh. *Corresponding author. E-mail: kumarajoy.cu@gmail.com or unescochakma@gmail.com

High-speed computing, large-capacity data communication, storage, processing, electronic devices are essential objects for the development of the national economy and national security. The basic and supporting materials have required for the production of electronic circuits, such as large circuits, flat display devices, compound semiconductor devices, solar cells, and optical fibers [3, 4]. Regarding this case, the use of semiconductors has been increasing day by day, and the role of semiconductors is related to the field of discovering new advanced technologies for electronic devices. The downstream IC, LCD/LED, BJT, MOSFET, transistor, resistor, and photovoltaic solar power are almost impossible to produce without the semiconductors [5, 6]. The semiconductor device is just a name of insulating with a small band gap, and the range of band gap is 3.0 to 1.0 eV. Due to their enormous applications in the computer devices, photovoltaic industry, transistors, lasers, solar cells demand and development, its researches have been spreading recent times, as well as industrial applications [7].

The discovery of new devices and existing materials for futuristic electronic devices is an essential area of research in the advanced subject of material science and engineering. The most common semiconductors are GaAs, InN, GaN, and ZnTe, while ZnO is considered as the best understood through band gap concepts. The elements of groups IV and VI have traditionally been used for the metal oxides and crystal-based semiconductors, and the most common elements are Te, Zn, Cu, Si, Ge, Sn, and Se for their easily electronic transition from valance band to conduction band [8, 9]. Secondly, the enormous demand in the area of the electronic device makes the new searching material in engineering while alloys, some metal oxides and crystals, such as GaP, GaSb, CdSe and Cu_2S, etc have made the boarding scope in applications [10, 11]. Among all targeting materials, $AlCuO_2$ has been considered as a typical compound of semiconductor materials for potential applications as optical fiber, thermoelectric devices, photocatalyst, and catalytic properties, which have lead to speedy progress in techniques and methods. In addition, $AlCuO_2$ has been using to create thin films [12], a catalyst for hydrogen production for organic or dye degradation [13], dye-sensitized photocathode [14], strain to tailor electronic [15], powder dispersed in composite gel electrolyte in the solar cell [16] and bulk single crystals, as well as in areas of electronic ceramic reinforcement, semiconductor material synthesis, and plastics or aluminum/copper matrix alloy production [7, 17, 18]. Moreover, $AlCuO_2$ had known as the delafossite oxides, which are transparent p-type semiconductor in the thin-film form [19].

Despite these many advanced applications, much of the confusion has arisen from conflicting reports on the band gap which was measured by room temperature absorption techniques [20]. Some experimental reports for band gap had published from 1994 to 2009, whereas the band gap had an estimated 1.60 to 1.80 eV corresponding visible range around 348-400 nm [14, 21-23]. In our investigation, the band gap was determined by the simulation method using computational tools which supports less time and cost than experiments and compares the calculated band gap to the experiment value for its validation. Additionally, to develop and enhance its activity, Fe was doped on $CuAlO_2$, because Fe has already investigated as a medium atom for reducing the band gap, conductivity, and enhancing photocatalytic activity [24-31]. As the low-cost delafossite $CuAl_{0.96}Fe_{0.04}O_2$ had firstly synthesized and introduced as the material of thermoelectric properties, there are not enormous study on $CuAl_{0.96}Fe_{0.04}O_2$ (32).

For this view, the other aim of this study is to examine the effect of Fe doped replacing Cu on the $AlCuO_2$ compound, and its molecular formula becomes $AlCu_{0.96}Fe_{0.04}O_2$ after 4% Fe doping. As a result, these properties, which have been derived from simulation after doping, have significant intensive attention for potential applications. For using the $AlCuO_2$, this study supports to development of the theoretical concept using the first principle study and opens a new window for potential application by Fe doping in $AlCuO_2$.

2. Results and Discussion

2.1 Optimized structure

The lattice parameters are a= 2.880Å, b = 2.880Å, c = 11.413Å and angels between them as α= 90.0 A°, β= 90.0 A°, γ= 120.0 A°. The monoclinic $AlCuO_2$ crystal and also the area cluster is Hermanna Mauguin, P63/mmc, hexagonal crystals system, point cluster 6/mmm, hall-P 6c 2c, density 4.96 g/cm3 shown in Figure 1a, and also the Fe doped optimized structure is addressed in Figure 1b.

2.2 Electronic band structure

To determine the electronic band structure of $AlCuO_2$ and $AlCu_{0.96}Fe_{0.04O2}$, the Fermi energy level was set at zero. From Figure 2a for $AlCuO_2$ semiconductor, the minimum of conduction (MCB) was obtained at the G symmetry point, whereas the maximum of valance bands (MVB) was also found at G symmetry points. As the MCB and MVB are obtained at point G symmetry point, it is called an indirect band gap, and it is calculated by 1.81 eV. It also seems that each of the higher and lower components of the conduction band is well dispersed in the near G, Z, and X symmetry points than F and L symmetry points. The calculated band gap of 1.81 eV is completely overlapped with the experimental band gap reported by Lu, Yun, et al. [33] which was 1.80 eV. On the other hand, the higher level of the valence band is close to the G symmetry point, and it is equally dispersive. Another point is that the lower part is not well dispersive like the upper level. In general, a lower carrier effective mass corresponds to the next carrier mobility. The main key point of this research is noted that the band gap of $AlCuO_2$ has been reduced for use as a superconductor when Fe had doped by 4%. The reason is explained that Fe atom can enhance the electron density in both areas of valance band and conduction band besides d and p orbitals of Fe atom have quickly overlapped with the p and d orbitals with Al and Cu metals for quickly transferring the hole electrons. That is why the minimum portion of Fe by 4% was doped in $AlCuO_2$ and illustrated the effect on the band structure. The band gap was recorded at the middle of the G and Y symmetry point for both MCB and MVB after doping, showing a direct band gap by 0.00 eV, which stands for that Fe atom has a high capacity on $AlCuO_2$ to reduce the band gap acting for a superconductor.

2.3 The Density of states and Partial density of state

The density of the state indicates the characteristic of electronic band structures and the splitting of an orbital. The GGA with PBE method was used to calculate the density of states (DOS) of Al, Cu, Fe, and O atoms of $AlCuO_2$ and $AlCu_{0.96}Fe_{0.04O2}$ crystals. Form Figure 3b, the sum of DOS for $AlCuO_2$ consists of 2s, 2p orbitals for an oxygen atom, 3s, 3p orbitals for aluminum, and 4s, 3d orbitals for Cupper atom.

Similarly, after Fe doping by 4%, the sum of DOS composes of 2s, 2p orbitals for an oxygen atom, 3s, 3p orbitals for aluminum and 4s, 3d orbitals for Cupper and 3d, 4s orbitals for Iron atom. From Figure 3a, it is observed that the DOS of $AlCuO_2$ in the valance band is much smaller than the DOS of $AlCu_{0.96}Fe_{0.04O2}$. Secondly, the DOS of $AlCu_{0.96}Fe_{0.04O2}$ in the conduction band is almost three times greater than the DOS of $AlCuO_2$. The DOS of the valance band is found at 65 electron/eV, while the DOS of the conduction band is recorded at about 30 electron/eV. To compare the s, p, and d orbitals for both doping and undoped $AlCuO_2$, the orbitals for $AlCu_{0.96}Fe_{0.04O2}$ are much higher than $AlCuO_2$, and it can be said that the Fe doping on $AlCuO_2$ has increased the DOS of any crystal showing in figures 3a, 3b, 3c, 3d, 3e, and 3f.

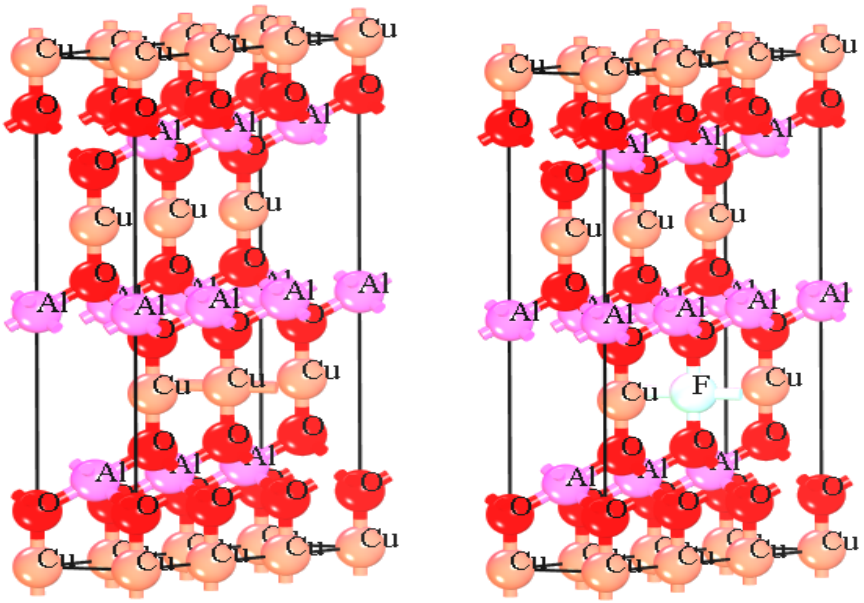

(a) (b)

Fig. 1. (a) Structure for $AlCuO_2$. (b). Structure for $AlCu_{0.96}Fe_{0.04}O_2$.

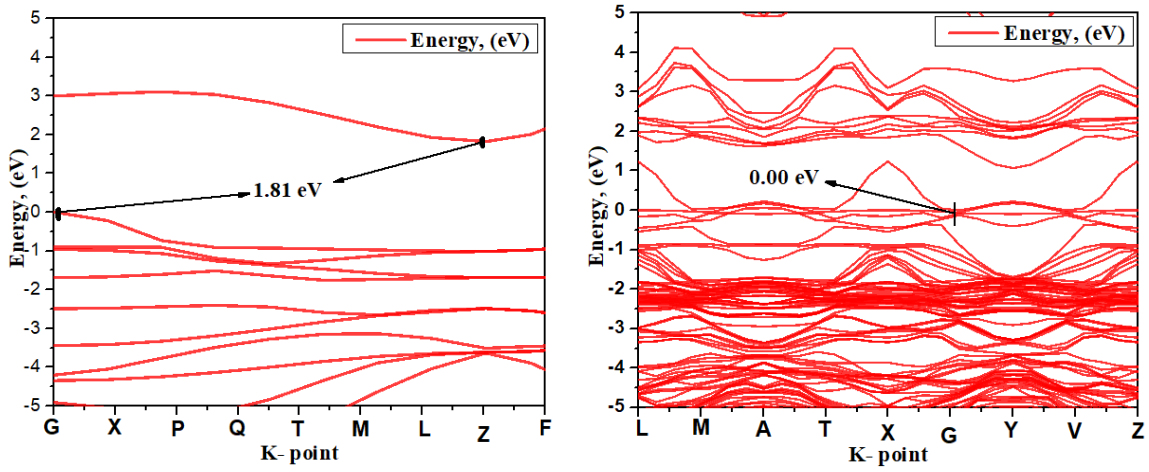

(a) (b)

Fig. 2. (a) Electronic structure for undoped. (b) Electronic structure for doped.

2.4 Optical properties

2.4.1 Optical reflectivity

The study and characterization of optical reflectivity for $AlCuO_2$ and $AlCu_{0.96}Fe_{0.04O2}$ consist of the intense light first inducing a nonlinear response in a medium. The medium is reacting and modifying the optical fields of the nonlinear method. There is a wide variety of nonlinear optical phenomena in semiconductors, which leads to much identification showing a sharp peak on the subject of nonlinear properties. At first, we go through the quantification of optical reflectivity of a crystalline material because it has a significant role in the electronic transition from the valance band to the conduction band of compounds. The amount of light that is incident on the surface of the semiconductor materials, and it is estimated from the reflectivity data, mentions the higher electronic transition. Withal, it is related to the absorbance of that materials. In our investigation, we observed that the optical reflectivity was found as a sharp peak at 2, 7, 13, 22, and 24 for doping and 5, 8, 12, 22, and 24 photon energy while both doping and undoped overlap at 24 eV photon energy, and doping is slightly higher than undoped as illustrated in Figure 4.

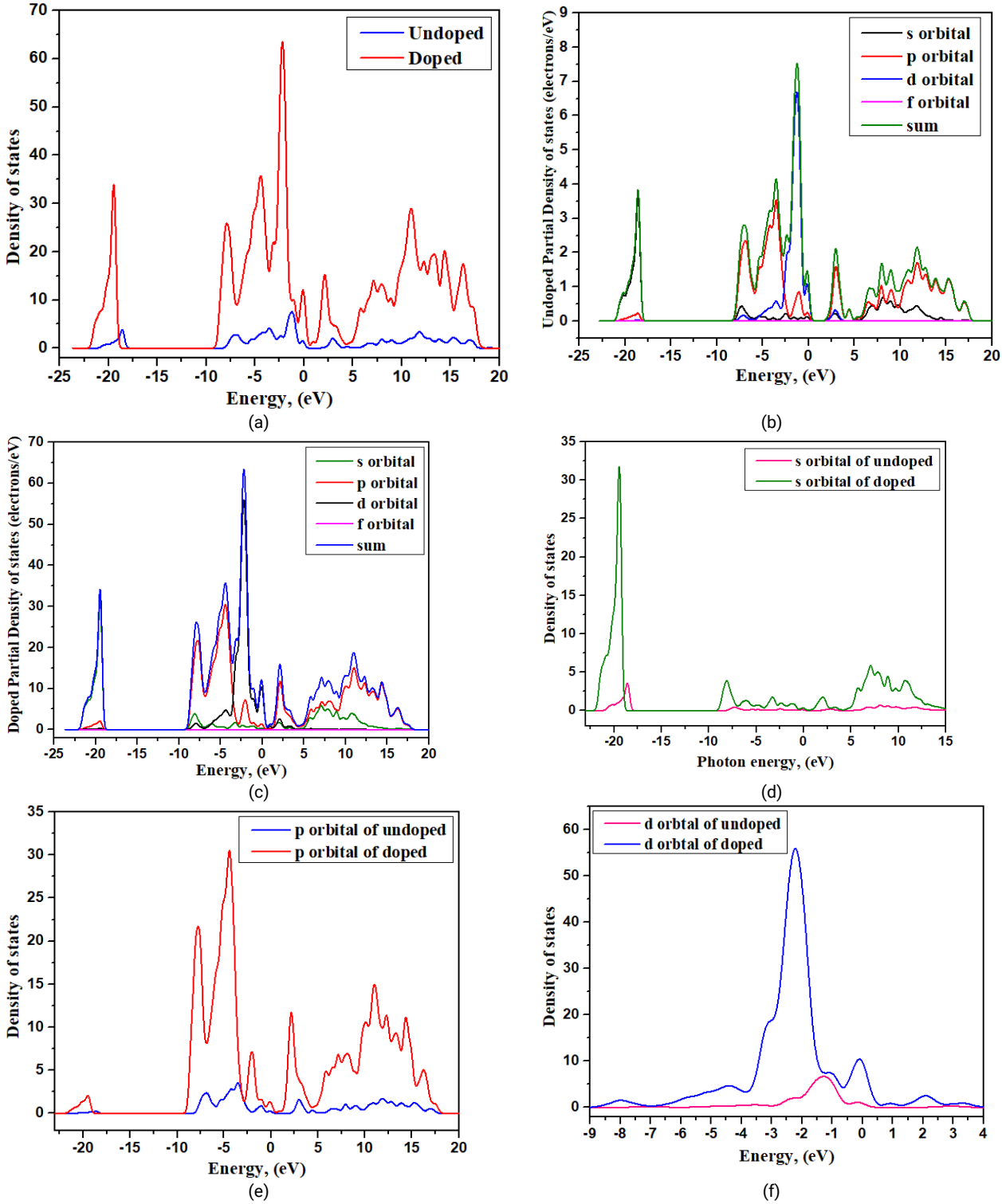

Fig. 3. (a) comparison of total DOS for doped and undoped; (b). PDOS for undoped; (c). PDOS for doped; (d). a comparison of the DOS of s orbital for doped and undoped; (e). a comparison of the DOS of p orbital for doped and undoped; f). a comparison of the DOS of d orbital for doped and undoped.

2.4.2 Absorption

The polycrystalline polarization method is utilized to calculate the optical absorbance of the $AlCuO_2$ and $AlCu_{0.96}Fe_{0.04}O_2$ materials. During the simulation, a small smearing value of 0.1 was applied to attain more distinguishable absorbed peaks. The obtained absorbed peaks are attributed to the photo transition energies from the maximum valance band (MVB) to the minimum conduction band (MCB) under visible light irradiation represented in Figure 5, which indicates that this material can absorb photons of visible range. Moreover, it has been observed that the absorption of $AlCu_{0.96}Fe_{0.04}O_2$ is almost higher than $AlCuO_2$ except for the range of 5 to 10 eV. Fe doping can increase absorption than its parent material.

2.4.3 Reflective Index

The refractive index of a material is an impactful parameter for measuring photon absorption. The large value of the refractive index is associated with the greater denser medium. Figure 6 displays the refractive index as a function of photon energy where the real part and the imaginary part

are mentioned for both of the undoped and doped, and it shows an inverse pattern. The real and imaginary part of doping is higher than undoped consecutive at all photon energy, which means that after Fe doping, $AlCu_{0.96}Fe_{0.04O2}$ can act as a denser medium than $AlCuO_2$.

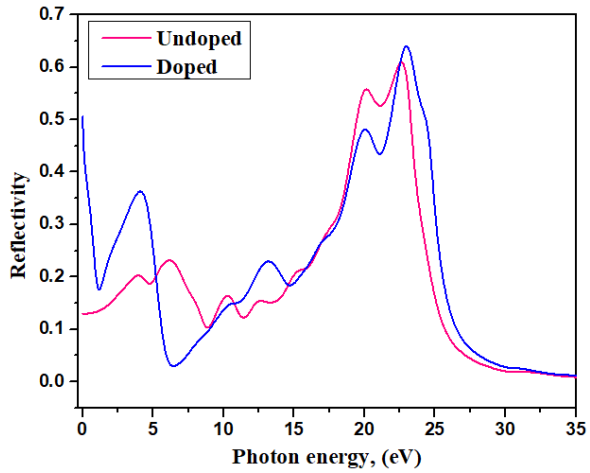

Fig. 4. Reflectivity.

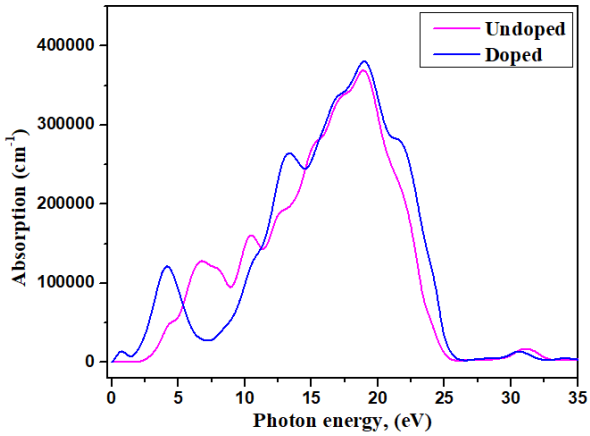

Fig. 5. Absorption.

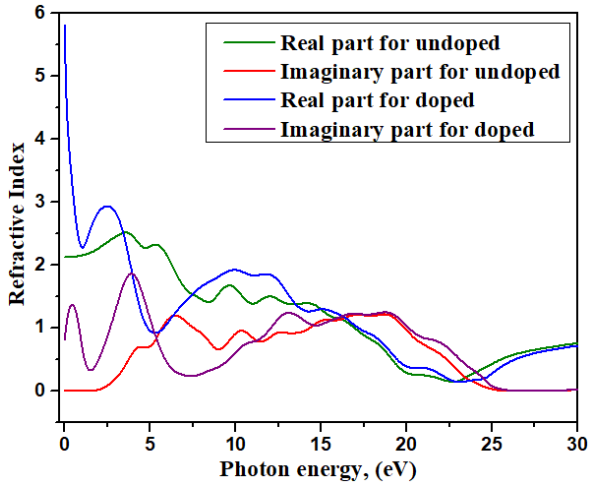

Fig. 6. Refractive index.

2.4.4 Dielectric Function

The dielectric function is an essential tool to investigate their optical properties, which are related to adsorption properties as the following equation for solid [34].

$$\varepsilon = 〖\varepsilon〗_1(\omega)+i〖\varepsilon〗_2(\omega)$$

Where, $\varepsilon 1$ (ω) and $\varepsilon 2$ (ω) are denoted the dielectric constant (real part) and the dielectric loss factor (imaginary part), respectively. The dielectric function has a relationship with the space of materials, which are physically equivalent to the permittivity or absolute permittivity. The real part of the dielectric function represents the energy storage capability in the electric field, and from Figure 7, it has been seen that the real part of the dielectric function has declined after Fe doping. As a result, the conductivity was soared in $AlCu_{0.96}Fe_{0.04O2}$ than $AlCuO_2$.

The second symbol ($\varepsilon 2$ (ω)) from the above equation is known as the imaginary part, which represents the energy dissipation capability of the dielectric materials. From Figure 7, the imaginary part of undoped is less than doping.

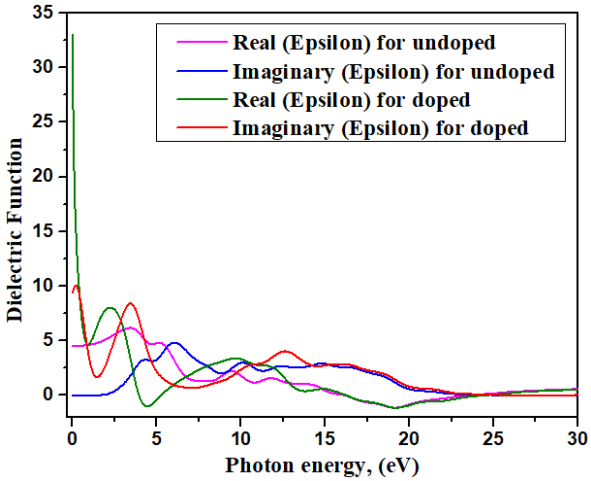

Fig. 7. Dielectric function.

2.4.5 Conductivity

The conductivity of the semiconductor-based materials in terms of the energy band and orbital electrons is linked with the discrete space of electrons in orbitals. This is also produced due to the presence of holes and free electrons in the crystal molecules. From Figure 8, it is observed that the conductivity for both real and imaginary parts is bigger than the undoped of $AlCuO_2$.

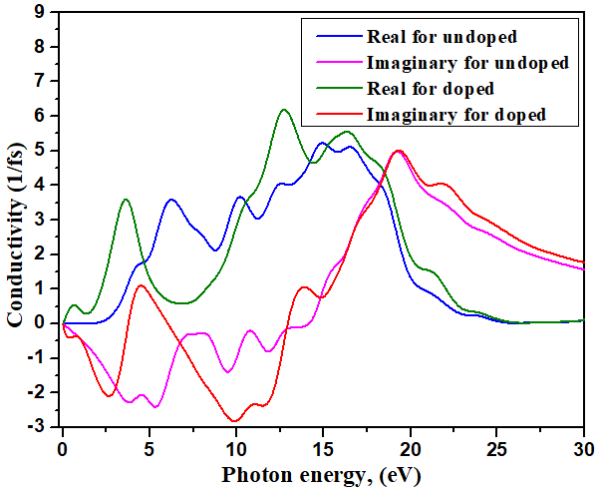

Fig. 8. Conductivity.

2.4.6 Loss function

There are two regions for the electronic energy loss function, such as the high energy region or low energy region for optical properties. From Figure 9, the loss function for doped is poor higher than undoped.

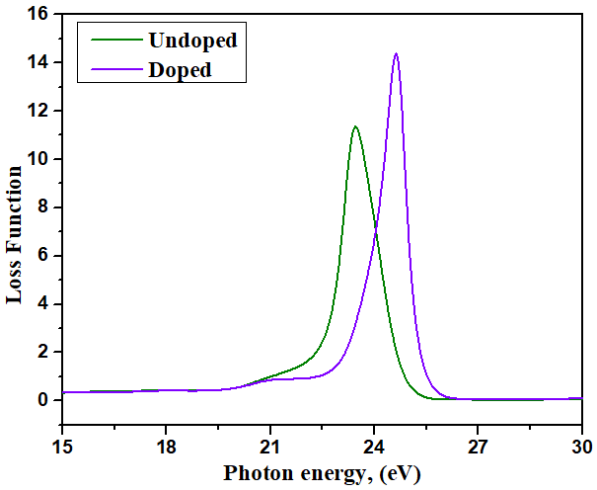

Fig. 9. Loss function.

3. Material and Methods

At first, the geometric optimization was achieved, and the convergence criterion for the force between atoms, the maximum displacement, and the total energy was built in 2×10^{-6} eV/atom, 1×10^{-5}A°, and 1×10^{-5} eV/atom, respectively. The 1×1×1 supercell models were considered to simulate the structural electronic and optical properties of $AlCuO_2$ and $AlCu_{0.96}Fe_{0.04}O_2$ shown in Figure 1a and Figure 1b, respectively. To calculate the band gap and density of states, the method of GGA with PBE was optimized using CASTEP code [33] from material studio 8.0 [34]. In this condition, the band gap and density of states were calculated using the method of GGA with PBE, keeping the cut off at 523 and k point at 4×4×2 with nom-conserving pseudopotentials functional. The optical properties, such as refractive index, reflectivity, absorption, conductivity, and loss function, were also calculated using the same method and condition.

4. Conclusions

The electronic structure and optical properties of $AlCuO_2$ and Fe doped by 4% in $AlCuO_2$ have theoretically and computationally investigated for establishing a comparing data of doped and undoped. First of all, the band gap of $AlCuO_2$ has been recorded by 1.81 eV as supporting a semiconductor that has been filled up the lack of literacy about band gap and electronic structure for $AlCuO_2$ of a theoretical result. The main novelty of this study is to evaluate the Fe doping effect on electronic structure, especially band gap, DOS, PDOS, and optical properties. After Fe doping by 4 % in $AlCuO_2$, the band gap has shifted in 0.00 eV, and PDOS and sum of DOS have increased, as well as the delocalization of electron has also been enhanced. Secondly, the optical properties, due to Fe doping, has changed. The optical absorption, reflectivity, loss function, and conductivity of doped $AlCuO_2$ are greater than undoped $AlCuO_2$, but the real part of the dielectric function is lower than undoped. Finally, it can be said that the 4% Fe doping in $AlCuO_2$ converts into a superconductor from a wide band gap semiconductor.

Acknowledgments

Authors offer the thankful to Md Jahidul Islam, Lecturer, Department of Physics, European University of Bangladesh for his cordial supports and Tomal Hossain for his technical help.

Author Contributions

The optimization, working procedure and data analysis were done by Md. Tawhidul Islam, Unesco Chakma, Debashis Howlader. Unesco Chakma wrote the draft of manuscript. Ajoy Kumer supervised and designed this project and wrote this manuscript.

References and Notes

[1] Izatt, R. M. I.; Steven, R.; Bruening, R. L.; Izatt, N. E.; Moyer, B. A. *Chem. Soc. Rev.* **2014**, *43*, 2451. [Crossref]

[2] Chacko, E. *GeoJournal* **2007**, *68*, 131. [Crossref]

[3] Zou, D.; Wang, D.; Chu, Z.; Lv, Z.; Fan, X. *Coord. Chem. Rev.* **2010**, *254*, 1169. [Crossref]

[4] Song, Y. K.; Stein, J.; Patterson, W. R.; Bull, C. W.; Davitt, K. M.; Serruya, M. D.; Zhang, J.; Nurmikko, A. V.; Donoghue, J. P. *J. Neural Eng.* **2007**, *4*, 213. [Crossref]

[5] Baeg, K. J.; Caironi, M.; Noh, Y. Y. *Adv. Mater.* **2013**, *25*, 4210. [Crossref]

[6] Fortunato, E.; Barquinha, P.; Martins, R. *Adv. Mater.* **2012**, *24*, 2945. [Crossref]

[7] Bosi, M.; Pelosi, C. *Prog. Photovoltaics* **2007**, *15*, 51. [Crossref]

[8] Cohen, M. H.; Falicov, L. M.; Golin, S. *IBM J. Res. Dev.* **1964**, *8*, 215. [Crossref]

[9] McMahon, M. I.; Nelmes, R. J. *Phys. Status Solidi B* **1996**, *198*, 389. [Crossref]

[10] Kim, S.; Fisher, B.; Eisler, H. J.; Bawendi, M. *J. Am. Chem. Soc.* **2003**, 125, 11466. [Crossref]

[11] Lu, M. Y.; Hong, M. H.; Ruan, Y. M.; Lu, M. P. *Chem. Comm.* **2019**, *55*, 5351. [Crossref]

[12] Kawazoe, H.; Yasukawa, M.; Hyodo, H.; Kurita, M.; Yanagi, H.; Hosono, H. *Nature* **1997**, *389*, 939. [Crossref]

[13] Qing, S.; Hou, X.; Liu, Y.; Li, L.; Wang, X.; Gao, Z.; Fan, W. *Chem. Comm.* **2018**, *54*, 12242. [Crossref]

[14] Benko, F. A.; Koffyberg, F. P. *J. Phys. Chem. Solids* **1984**, *45*, 57. [Crossref]

[15] Witkoske, E.; Guzman, D.; Feng, Y.; Strachan, A.; Lundstrom, M.; Lu, N. *J. Appl. Phys.* **2019**, *125*, 082531. [Crossref]

[16] Suriwong, T.; Thongtem, T.; Thongtem, S. *Mater. Sci. Semicond. Process.* **2015**, *39*, 348. [Crossref]

[17] Deng, Z.; Zhu, X.; Tao, R.; Dong, W.; Fang, X. *Mater. Lett.* **2007**, *61*, 686. [Crossref]

[18] Koriche, N.; Bouguelia, A.; Aider, A.; Trari, M. *Int. J. Hydrogen Energy* **2005**, *30*, 693. [Crossref]

[19] Warner, M.; Din, S.; Tupitsyn, I. S.; Morley, G. W.; Stoneham, A. M.; Gardener, J. A.; Wu,

Z.; Fisher, A. J.; Heutz, S.; Kay, C. W. M. *Nature* **2013**, *503*, 504. [Crossref]

[20] Bhuiyan, A. G.; Sugita, K.; Kasashima, K.; Hashimoto, A.; Yamamoto, A.; Davydov, V. Y. *Appl. Phys. Lett.* **2003**, *83*, 4788. [Crossref]

[21] Yanagi, H.; Inoue, S. I.; Ueda, K.; Kawazoe, H.; Hosono, H.; Hamada, N. *J. Appl. Phys.* **2002**, *88*, 4159. [Crossref]

[22] Tate, J.; Ju, H. L.; Moon, J. C.; Zakutayev, A.; Richard, A. P.; Russell, J.; McIntyre, D. H. *Phys. Rev. B* **2009**, *80*, 165206. [Crossref]

[23] Nie, X.; Wei, S. H.; Zhang, S. B. *Phys. Rev. Lett.* **2002**, *88*, 066405. [Crossref]

[24] Chakma, K. B.; Kumer, A.; Chakma, U.; Howlader, D.; Islam, T. *Int. J. New Chem.* **2020**, *4*, 24. [Crossref]

[25] Chakma, U.; Kumer, A.; Chakma, K. B.; Islam, T.; Howlader, D. *Adv. J. Chem., Sect. A* **2020**, *3*, [Crossref]

[26] Islam, M. J.; Kumer, A. *SN Appl. Sci.* **2020**, *2*, 251. [Crossref]

[27] Chakma, U.; Kumer, A.; Chakma, K. B.; Islam, T. Howlader, D. *Adv. J. Chem., Sect. A* **2020**, *3*, 542. [Crossref]

[28] Hasan, M. M.; Kumer, A.; Chakma, U. *Adv. J. Chem., Sect. A* **2020.** *In Press* [Link]

[29] Kamal, B. C.; Kumer, A.; Chakma, U.; Howlader, D.; Islam, T. *Int. J. New Chem.* **2020**, *7*, 247. [Crossref]

[30] Chakma, U.; Kumer, A.; Chakma, K. B.; Islam, T.; Howlader, D.; Mohamed, R. M. K. *Eurasian Chem. Commun.* **2020**, *2*, 573. [Crossref]

[31] Hasan, M.; Kumer, A.; Chakma, U.; Islam, T. *Mol. Simul.* **2021**, *47*. [Crossref]

[32] Siriwongrungson, V.; Sakulkalavek, A.; Sakdanuphab, R. *J. Mater. Sci.: Mater. Electron.* **2016**, *27*, 11102. [Crossref]

[33] Clark, S. J.; Segall, M. D.; Pickard, C. J.; Hasnip, P. J.; Probert, M. J.; Refson, K.; Payne, M. C. *Z. Kristallogr.* **2005**, *220*, 567. [Crossref]

[34] Perdew, J. P.; Burk, K.; Ernzerhof, M. *Phys. Rev. Lett.* **1996**, *77*, 3865. [Crossref]

How to cite this article

Islam, T.; Kumer, A.; Chakma, U.; Howlader, D. *Orbital: Electron. J. Chem.* **2021**, *13*, 58.
http://dx.doi.org/10.17807/orbital.v13i1.1533